Use of a Least Squares Finite Element Lattice Boltzmann Method to Study Fluid Flow and Mass Transfer Processes

Yusong Li, Eugene J. LeBoeuf, and P.K. Basu

Department of Civil and Environmental Engineering
Vanderbilt University, Nashville,
Tennessee 37325

Abstract. In our previous efforts, a least squares finite element lattice Boltzmann method (LSFE-LBM) was developed and successfully applied to simulate fluid flow in porous media. In this paper, we extend LSFE-LBM to simulate solute transport in bulk fluid and couple it with non-linear sorption/desorption processes at solid particle surfaces. The influences of the Peclet number and sorption non-linearity on solute transport is evaluated. Results of this work demonstrate the capability of using LSFE-LBM to study fluid flow and non-linear mass transfer processes at the pore scale.

1 Introduction

To provide for effective and efficient groundwater contamination prevention and remediation, it is important to possess a clear understanding of the complex mass transfer processes governing solute transport in the subsurface environment. Solute mass transfer in the subsurface includes several processes acting simultaneously: (i) advective-dispersive transport from bulk solution to the boundary layer of a soil or sediment particle; (ii) film diffusion across adsorbed water to the surface of a particle; (iii) sorption/desorption processes at the surface of the soil particle; and (iv) intrasorbent diffusion. Different factors, including transport-related non-equilibrium processes and sorption-related non-equilibrium processes, influence mass transfer in the subsurface [1], leading to non-ideal behaviors; i.e., early breakthrough and tailing breakthrough curves (BTC). Traditional advective-dispersive equations, which employ a local equilibrium assumption (LEA), fail to predict this non-ideal behavior [2]. In the last two decades, many efforts were devoted to better capture both transport-related and sorption-related non-equilibrium processes and elucidate the comparative contributions of different factors [3].

Recently, lattice Boltzmann method has been successfully applied to simulate fluid flow in porous media [4], providing a powerful alternative to model transport-related non-equilibrium processes. In this paper, we use a newly developed least squares finite element lattice Boltzmann method [5] to simulate fluid flow in porous media. Further, we extend LSFE-LBM to simulate solute transport in bulk fluid and couple it with non-linear sorption/desorption processes at particle surfaces.

V.S. Sunderam et al. (Eds.): ICCS 2005, LNCS 3514, pp. 172 – 179, 2005.

2 Least Squares Finite Element Lattice Boltzmann Method

Although LBM has been developed as an effective tool to simulate complex fluid flow problems in porous media, one of the challenges with LBM is its inability to allow irregularity in the lattice [6]. We developed a least squares finite element lattice Boltzmann method (LSFE-LBM), which uses a LSFE method [7] in space and Crank-Nicolson method in time to solve the lattice Boltzmann equation. As described in an earlier publication [5], LSFE-LBM was successfully implemented on unstructured mesh to simulate fluid flow in porous media, requiring fewer grid points and consuming significantly less memory than traditional LBM.

2.1 Derivation of LSFE-LBM

Beginning with the basic equations of the LBM with a Bhatnagar-Gross-Krook collision operator:

$$\frac{\partial f_i}{\partial t} + \vec{c}_i \cdot \vec{\nabla} f_i = -\frac{1}{\tau}(f_i - f_i^{eq}) \qquad (i = 1,2,...N) \tag{1}$$

where f_i represents particle distribution moving with velocity c_i, τ is the relaxation time, f_i^{eq} is the local equilibrium function, and N is the number of elements per site based on the LB model employed. Discretizing in time with a Crank-Nicholson scheme, a standard form of the governing equation for LSFE-LBM is

$$Lf^{n+1} = p \tag{2}$$

where the differential operator

$$\begin{aligned} L &= c_x \frac{\partial}{\partial x} + c_y \frac{\partial}{\partial y} + A \\ A &= \frac{2}{\Delta t} + \frac{1}{\tau} \\ p_i &= (\frac{2}{\Delta t} - \frac{1}{\tau}) f_i^n + \frac{1}{\tau}(f_i^{eq,n+1} + f_i^{eq,n}) - (c_x \frac{\partial f_i^{n+1}}{\partial x} + c_y \frac{\partial f_i^{n+1}}{\partial y}) \end{aligned} \tag{3}$$

where Δt denotes the time step in the Crank-Nicholson scheme.

In the finite element implementation, the problem domain is first discretized into a set of finite elements, and then an approximate solution, $f_h^{e,n+1}$ in the eth finite element is formulated as:

$$f_h^{e,n+1} = \sum_{j=1}^{n} N_j f_j^{n+1} \tag{4}$$

Here, N_j denotes the element shape function, n represents the number of variables in the element, and f_j is the value of the j-th variable. Introducing this approximation into Eq. (2), the residual error at a point in the element is obtained. Integrating the square of this error over each element and minimizing the integral with respect to the nodal variables of the element, the elemental matrix relationship of the following form is obtained:

$$K_e F_e^{n+1} = P_e \tag{5}$$

where $K_e = \int_{\Omega_e} Q^T Q d\Omega_e$ with the i^{th} element of Q,

$$Q^i = c_x \frac{\partial N_i}{\partial x} + c_y \frac{\partial N_i}{\partial y} + AN_i \tag{6}$$

F_e^{n+1} is the vector of nodal values at the current time step, and

$$P_e = \int_{\Omega_e} Q^T p_h^e d\Omega_e \tag{7}$$

Here, the K_e matrix is symmetric and positive definite.

2.2 LSFE-LBM Simulating Fluid Flow

In this study, a two-dimensional, nine-velocity lattice model (D2Q9) [8] is employed to implement LSFE-LBM for fluid flow. Accurate numerical results have been obtained for incompressible Poiseuille flow, Couette flow, and flow past a circular cylinder. Figure 1 is an example application of LSFE-LBM modeling fluid flow in porous media using an unstructured mesh.

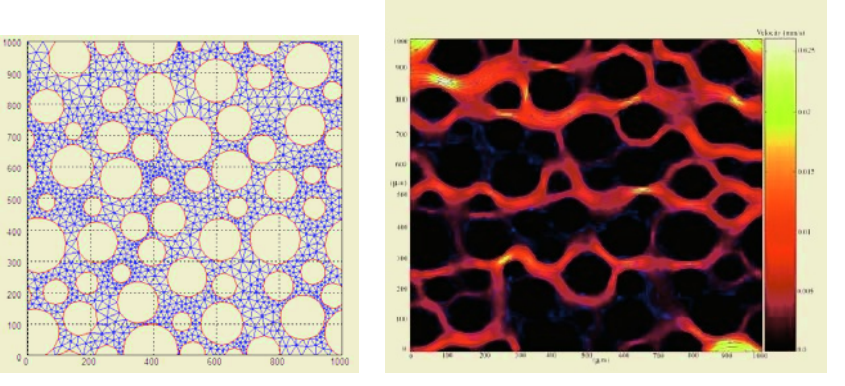

Fig. 1. LSFE-LBM-based unstructured mesh and velocity vectors for fluid flow in porous media

2.3 LSFE-LBM Simulating Solute Transport

In this study, we assume that the solute concentration is sufficiently low that it will not influence solvent flow. In this case, the solute can be described by a separate particle distribution function [9]. To recover the advection-diffusion equation, a simple square lattice with four possible directions is sufficient, which is thus used for implementing LSFE-LBM simulating solute transport.

The validation of LSFE-LBM simulating solute transport is evaluated by a problem describing diffusion between two parallel walls. As illustrated in Figure 2, the two walls are assumed to be porous and a constant normal flow u_a is injected through the lower wall and removed from the upper wall. The concentration of solute at the lower and upper walls is maintained with C_U and C_L, respectively. In this specific problem, C_U is assumed higher than C_L; it follows that solute diffuses counter to the flow of the fluid.

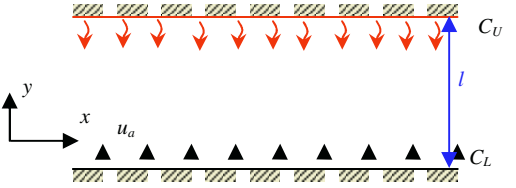

Fig. 2. Diffusion between two parallel walls

The governing equation for this problem is:

$$\frac{\partial \Phi}{\partial t} = D\frac{\partial^2 \Phi}{\partial y^2} + u_a \frac{\partial \Phi}{\partial y} \tag{8}$$

$$\Phi(y,0) = 0, \qquad \Phi(0,t) = 0, \qquad \Phi(l,t) = 1 \tag{9}$$

where, Φ is a normalized concentration defined as: $\Phi = \dfrac{C - C_L}{C_U - C_L}$, and D is the diffusivity of solute. Analytical solutions can be obtained for this problem in two special cases. In Case I, when $u_a = 0$, Eq. (8) will reduce to an unsteady state pure diffusion problem. The analytical solution can be expressed as:

$$\Phi(y,t) = \frac{y}{l} + \frac{2}{\pi}\sum_{n=1}^{\infty}\frac{(-1)^n}{n}\sin\frac{n\pi y}{l}e^{-n^2 t/\lambda}, \text{ where } \lambda = \frac{l^2}{\pi^2 D} \tag{10}$$

When $u_a \neq 0$ (Case II), analytical solutions are only available for steady-state conditions:

$$\Phi = \frac{Exp(u_a y / D) - 1}{Exp(u_a / D) - 1} \tag{11}$$

Results presented in Figure 3 illustrate that LSFE-LBM achieves close agreement with the analytical solution for solute transport in both unsteady state and steady state conditions.

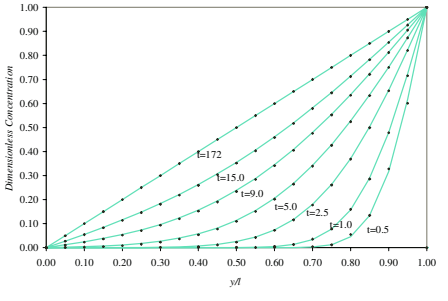

(a)

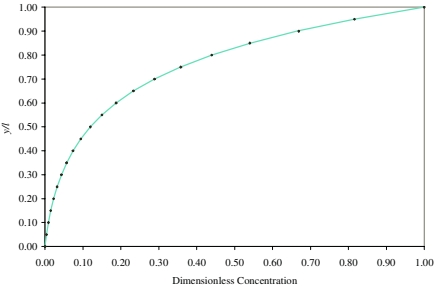

(b)

Fig. 3. Comparison of LSFE-LBM solution (points) and analytical solution (line) for diffusion between two parallel walls. (a) represents unsteady state solutions when water velocity u_a=0 and (b) represents steady state solution when water velocity $u_a \neq 0$

3 Mass Transfer Processes Simulation

3.1 Problem Description

To explore the influences of different factors on mass transfer processes, we consider fluid flow and transport through and around a single circular particle, set in a two-dimensional domain with a uniform far-field velocity, as illustrated in Figure 4.

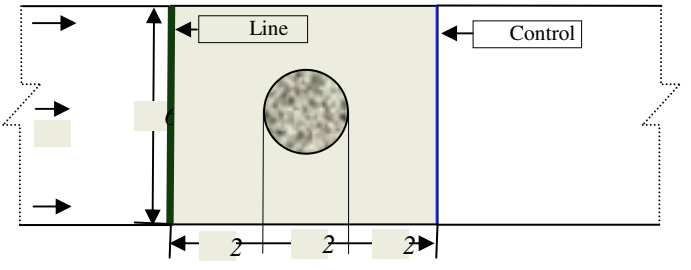

Fig. 4. An illustration of fluid flow and solute transport through and around a circular particle

A constant body force is imposed to drive fluid to flow from the left to right. When fluid flow reaches steady state, an instantaneous slug of solute is injected as a line source, as shown in Figure 4. Solute transport in the bulk fluid is driven by advection and diffusion processes. Several solute particles will diffuse across the water film to the surface of the particle. Sorption/desorption processes will then occur at the particle surface. The sorption rate at the particle surface can be expressed [10] as a function of the concentration difference between the solid and solution phases:

$$\frac{\partial q}{\partial t} = k_a C^n - k_d q \tag{12}$$

where, q is the solute concentration in the solid phase, C is the solute concentration in solution, k_a is a sorption rate coefficient, k_d is a desorption rate coefficient, and m is an exponent. At equilibrium, sorption isotherm models provide the relationship between sorbed-phase solute concentration and solute concentration in solution. Here, we express the relationship in terms of a Freundlich model:

$$q = (k_a / k_d) C^n = k_f C^n \tag{13}$$

3.2 Boundary Conditions

For fluid flow, periodic boundary conditions are imposed on all four boundaries, and a non-slip boundary condition is imposed at the solid surface. For solute transport, periodic boundary conditions are enforced at the top and bottom boundaries. Non-flux boundary conditions are enforced at the inlet and outlet of the simulation domain. In order to provide for a valid non-flux boundary condition, the length of the simulation domain is adjusted such that there is no mass loss at the domain inlet and outlet. At the solid particle surface, the boundary condition can be expressed as:

$$-D\frac{\partial C}{\partial n} = k_a C^n - k_d q \tag{14}$$

where D is the solute diffusion coefficient in the fluid, and n is the direction normal to the interface pointing toward the fluid phase. To implement this boundary condition in LSFE-LBM, a relationship between the concentration gradient and microscale particle parameters is required. For the 4 velocity lattice Boltzmann model, Eq. (15) can be derived by the Chapman-Enskog expansion.

$$\sum_i g_i c_{i\alpha} \cong C u_\alpha - \frac{\tau}{2} \partial_\alpha C \tag{15}$$

where g_i is the particle distribution function for the solute, and α denotes x and y axis directions for a two-dimensional case. Figure 5 provides an example of this boundary condition at the upper right quadrant of a circular particle.

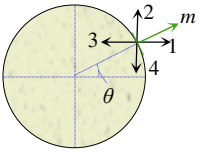

Fig. 5. A boundary node at the upper right part of the particle surface

Using Eq. (15), the following expressions are derived:

$$g_2 - g_4 = -(k_a C^n - k_d q) \sin\theta \tag{16}$$

$$g_1 - g_3 = -(k_a C^n - k_d q) \cos\theta \tag{17}$$

Further, we know:

$$g_1 + g_2 + g_3 + g_4 = C \tag{18}$$

Unknown distribution functions g_1 and g_2 is calculated, by solving this non-linear equation system. At each time step, the solid phase concentration, q, at the particle surface is updated based on Eq. (12).

3.3 Results

The simulation is carried out for a particle with radius R = 50 μm in the domain as defined in Figure 4. The evolution of the concentration profile is represented at four selected time steps in Figure 6. This example vividly displays the influence of particle geometry and fluid hydrodynamics on the solute concentration profile, suggesting the need to further evaluate transport-related non-equilibrium processes in more complex systems.

Using the same Reynolds number (Re = 1.0), we examined the influence of the Peclet number on mass transfer processes. (Pe = uL/D, where u is the x-direction specific flow rate, L is the characteristic length of the domain which equals six times the particle diameter, and D is the solute diffusion coefficient in the bulk fluid.) By adjusting the values of D, two different breakthrough curves for Pe=10 and Pe=20 are observed at the control plane (Figure 7(a)). While representing the relative speed of fluid flow and solute diffusion, a lower Pe value denotes further deviation from an ideal symmetric breakthrough, with an earlier breakthrough and longer tailing effect as indicated in Figure 7 (a).

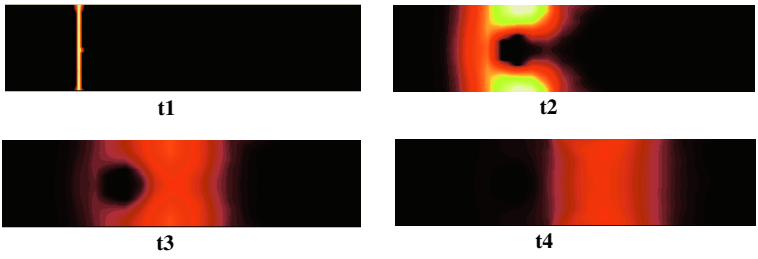

Fig. 6. Concentration profiles of a solute as it passes through and around a circular particle at four time points. Here t1 < t2 < t3 < t4

Further, the influence of non-linear sorption is evaluated to explore the influence of sorption-related non-equilibrium on the mass transfer processes. Keeping all the other parameters the same, we simulated two cases with n = 0.5 and n = 1.0 in the sorption rate equation (Eq. 12). Here, the evolution of solid phase concentration for a point at the surface of the particle is tracked. As expected, the presence of non-linear sorption (n = 0.5) leads to a much stronger tailing effect (Figure 7 (b)).

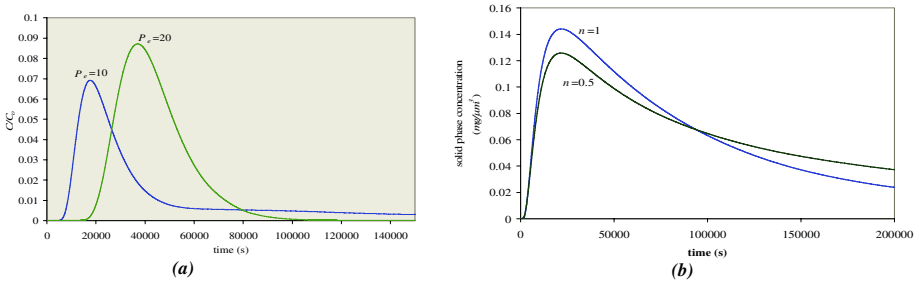

Fig. 7. (a) Breakthrough curves at the control plane for different P_e. (b) Time evolution of the solid phase concentration for a point at the surface of a particle

4 Conclusion

In this paper, we successfully applied our newly developed LSFE-LBM to simulate fluid flow and solute transport. LSEF-LBM was coupled with non-linear sorption/desorption through use of properly developed boundary conditions. The influences of particle geometry, Peclet number, and sorption/desorption non-linearity on solute transport were studied. Results from this work demonstrate the ability of LSFE-LBM to model fluid flow and highly non-linear mass transfer processes at the pore scale. In the future, LSFE-LBM will be applied to more complex systems to explore relative contributions of mass transfer processes with varying degrees of permeability and a variety of sorption/desorption properties.

References

1. M. L. Brusseau and P. S. C. Rao, Critical Reviews in Environmental Control 19, 33 (1989)
2. W. J. Weber and F. A. DiGiano, Process dynamics in environmental systems (John Wiley & Sons Inc., New York, 1996)
3. M. L. Brusseau, R. E. Jessup, and P. S. C. Rao, Water Resources Research 25, 1971 (1989).
4. S. Chen and G. D. Doolen, Annual Review of Fluid Mechanics 1998, 329 (1998)
5. Y. Li, E. J. LeBoeuf, and P. K. Basu, Physical Review E 69, Art. No. 065701 (2004)
6. J. D. Sterling and S. Chen, Journal of Computational Physics 123, 196 (1996)
7. B.-n. Jiang, The least-squares finite element method: theory and applications in computational fluid dynamics and electromagnetics (Springer, New York, 1998)
8. S. Succi, The Lattice Boltzmann equation for fluid dynamics and beyond (New York : Oxford University Press, 2001, 2001)
9. D. A. Wolf-Gladrow, Lattice-gas cellular automata and lattice Boltzmann models : an introduction (Springer, New York, 2000)
10. M. L. Brusseau and P. S. C. Rao, Geoderma 46, 169 (1990)